

Research Article

Reconciling Airborne Disease Transmission Concerns with Energy Saving Requirements: The Potential of UV-C Pathogen Deactivation and Air Distribution Optimization

Antoine Gaillard ¹, Detlef Lohse,^{2,3} Daniel Bonn,¹ and Fahmi Yigit ⁴

¹Van der Waals-Zeeman Institute, University of Amsterdam, Science Park 904, Amsterdam, Netherlands

²Physics of Fluids Group and Max Planck Center for Complex Fluid Dynamics, J. M. Burgers Centre for Fluid Dynamics, University of Twente, P.O. Box 217, Enschede 7500AE, Netherlands

³Max Planck Institute for Dynamics and Self-Organization, Am Fassberg 17, 37077 Göttingen, Germany

⁴Virobuster International GmbH, Köhlershohner Straße 60, 53578 Windhagen, Germany

Correspondence should be addressed to Antoine Gaillard; antoineogaillard@gmail.com and Fahmi Yigit; fahmi.yigit@virobuster.nl

Received 27 January 2023; Revised 22 May 2023; Accepted 1 July 2023; Published 16 August 2023

Academic Editor: Xiaohu Yang

Copyright © 2023 Antoine Gaillard et al. This is an open access article distributed under the Creative Commons Attribution License, which permits unrestricted use, distribution, and reproduction in any medium, provided the original work is properly cited.

The COVID-19 pandemic caused a paradigm shift in our way of using heating, ventilation, and air-conditioning (HVAC) systems in buildings. In the early stages of the pandemic, it was indeed advised to reduce the reuse and thus the recirculation of indoor air to minimize the risk of contamination through inhalation of virus-laden aerosol particles emitted by humans when coughing, sneezing, speaking, or breathing. However, such recommendations are not compatible with energy saving requirements stemming from climate change and energy price increase concerns, especially in winter and summer when the fraction of outdoor air supplied to the building needs to be significantly heated or cooled down. In this experimental study, we aim at providing low-cost and low-energy solutions to modify the ventilation strategies currently used in many buildings to reduce the risk of respiratory disease transmission. Measurements of the indoor air bacterial concentration in a typical office building reveal that ultraviolet germicidal irradiation (UVGI) modules added to the HVAC system are very efficient at inactivating pathogens present in aerosols, leading to indoor concentrations as low as outdoor concentrations, even with significant indoor air recirculation. Moreover, measurements of the CO₂ and aerosol air concentration reveal that, with air supply vents placed in the ceiling, placing the air exhaust vents near the floor instead of on the ceiling can improve the ventilation capacity in terms of effective flow rate, with significant consequences in terms of energy savings.

1. Introduction

Heating, ventilation, and air-conditioning (HVAC) systems aim at providing safety against high CO₂ and volatile organic compound (VOC) concentrations, as well as comfortable temperature and relative humidity levels, e.g., for employees working in office buildings as well as students and teachers in classrooms. With the COVID-19 pandemic, new hygienic concerns emerged and the importance of minimizing the risk of respiratory disease transmission in buildings was raised. Virus-laden airborne aerosols, which

are typically between 0.1 and 10 μm in size and remain in suspension in the air after being produced by humans when speaking, coughing, and sneezing [1–15], have indeed been found to be one of the major transmission routes of the SARS-CoV-2 virus and other viruses [16–26]. The risk of transmission therefore correlates with the rate at which indoor air is replaced by “clean” (outdoor or decontaminated) air by the building’s ventilation system. While only outdoor air supply was advised during the COVID-19 pandemic, with minimum indoor air recirculation to avoid aerosol spreading and accumulation [19], such strategy

clashes with sustainability requirements since the heating or cooling of outdoor air represents a large fraction of the total energy consumption of buildings, which is over one-third of society's global energy consumption [27]. Therefore, other solutions must be explored to reduce the risk of respiratory disease transmission in an ecologically acceptable way.

Historically, the first HVAC systems had minimal recirculation and maximum supply of outdoor air, offering a good protection against potential virus-laden aerosols, as well as CO₂ and potential organic volatile compounds (VOCs). After the first oil crisis, more indoor air recirculation was needed to reduce energy costs. This led to health problems referred to as the "sick building syndrome" such as eye and upper respiratory symptoms attributed to high CO₂ concentrations [28]. Generic air filters such as F5/F7 are often introduced to improve indoor air quality, but to trap all aerosols, finer HEPA filters are needed [29]. This suggests that, with insufficient air treatment, indoor air recirculation can lead to virus accumulation in buildings. Thermal wheels were therefore introduced in the 1990s to minimize recirculation and increase the supply of fresh air from outside, which is now heated by the warm exhaust air from the inside without physical contact between the two air streams. However, in addition to their high construction costs and maintenance levels, these energy recovery heat exchangers are known to leak and send some indoor air back into the building ("carry-over" effect) [30–32]. Hence, assuming that even a small fraction of virus recirculation is problematic, thermal wheels may not be the solution to optimize protection against viruses.

A promising solution for optimizing the hygienic quality of indoor air while keeping the economical and ecological benefits of air recirculation lies in the deactivation of pathogens via chemical [33], plasma [34, 35], or short ultraviolet (UV-C) [36, 37] air treatment. Air cleaning modules can either be inserted in the HVAC system to treat recirculating indoor air before it is reinjected into the room or can be added to the room in the form of mobile units. Recent studies suggest that plasma-based mobile air-cleaning units can be used to reduce aerosol concentrations in different conditions such as outpatient clinics [38] and gyms [39]. Ultraviolet germicidal irradiation (UVGI), which has first been used to purify (drinking) water during the fight against tuberculosis, for which Niels Ryberg Finsen received the Nobel Prize in Medicine in 1903, has also been used to purify air in operation rooms [40]. Since then, UVGI has been widely documented [41–44] and was proven effective also against coronaviruses [45, 46]. In the context of indoor air treatment, the effectiveness of UVGI cannot be tested by aerosol concentration measurements since UVGI can only deactivate pathogens contained in aerosols but does not remove aerosols from the air. However, in spite of its great potential, affordability, and low maintenance requirements, experimental studies on the efficiency of this technology in the context of indoor air quality in buildings are still lacking to date.

In addition to hygienic air treatment, the ventilation capacity is the key to reduce the risk of both short-range (via turbulent respiratory plumes emitted, e.g., when cough-

ing or sneezing [5, 47–49]) and long-range (after dilution and mixing in the room) disease transmission. In principle, long-range transmission can be reduced by increasing the ventilation power, which involves energy costs, or by improving the air distribution via wise placements of the air supply and exhaust vents to minimize pathogen concentrations in the breathing zone of occupants [27, 50–55]. In addition, future ventilation designs could rely on personalized ventilation concepts with clean air supplied near occupants [27, 56]. However, a key question that, to our knowledge, has not been addressed to date is whether the ventilation capacity, for example indexed by the CO₂ or aerosol elimination rate, can be improved by modifying the air distribution strategy.

In this experimental study, we explore the potential of (i) UVGI air treatment on the hygienic indoor air quality in an office building with partly recirculated indoor air and of (ii) air distribution optimization on the real ventilation capacity. Both aspects are aimed at providing further insights into finding low-cost and energy-saving solutions to adapt the ventilation systems currently used in many buildings, in order to reduce the risk of respiratory disease transmission. We start by reiterating a simple model correlating indoor CO₂ and aerosol concentrations with the ventilation capacity in Section 2. Our employed experimental methods are then presented in Section 3, and the results are presented in Section 4 and discussed in Section 5.

2. Model

The model derived in this section will be used in Section 4 to estimate the effective ventilation flow rate from CO₂ and aerosol concentration measurements. The room concentration of a gas or substance in suspension in the air, such as CO₂ or aerosols produced by humans (neglecting other sources), evolves over time and depends on the number of people present in the room and on the rate at which air is replaced by new (fresh or recirculated) air via the ventilation system. We recall here the simplest model for a well-mixed room [57] equivalent to a continuous stirred tank reactor [58] which assumes a homogeneous room concentration and which is the basis of the well-known Wells-Riley model for airborne disease transmission [59, 60]. Because of filtration (via face masks [61–63] or HEPA filters) and sedimentation-induced deposition on surfaces [3, 8, 49, 64, 65] affecting specifically airborne aerosols, the evolution in aerosol concentration may differ from that of CO₂ [66–70]. These effects are neglected here for simplicity and aerosols and CO₂ are treated equally. We also neglect the natural [64, 71–73] or active (via UVGI in our case) deactivation of pathogens contained in aerosols since we aim at describing the concentration of aerosols only and not that of active pathogens themselves.

The situation is described in Figure 1(a) where the air entering the room from supply vents consists of a fraction x of fresh outdoor air and a fraction $1 - x$ of recirculating indoor air captured by the exhaust vents before reentering the room after circulating through the AHU (air handling unit). The concentration C of either CO₂ or aerosols in a

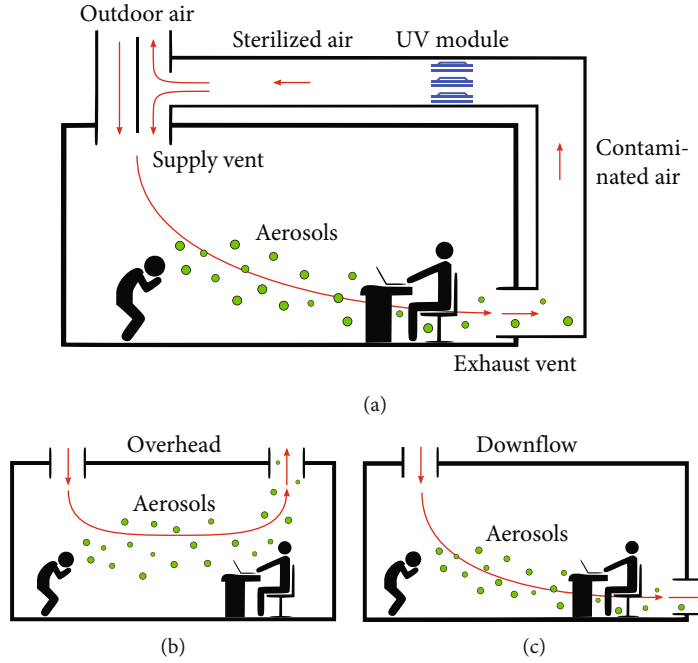


FIGURE 1: (a) Sketch of the ventilation system. (b, c) Sketch of the air flow (arrows) in an overhead (b) and downflow (c) air distribution strategies. Two employees are sketched, one producing aerosols (circles) via coughing or sneezing and the other potentially breathing them. Note that the specific case sketched here is not representative of all possible scenarios, e.g., with different positions of employees relative to supply and exhaust vents.

room of volume V with N people, each of them breathing at mass flow rate q , is set by the ventilation mass flow rate Q via the differential equation

$$\frac{dC}{dt} = \lambda[C_e - C + \alpha C_b], \quad (1)$$

where C_e and C_b are the CO_2 or aerosol concentrations in the outdoor air and in human breath, respectively. Here, we have introduced the air exchange rate

$$\lambda = \frac{xQ}{V}, \quad (2)$$

and the ratio

$$\alpha = \frac{Nq}{xQ}, \quad (3)$$

of people vs. ventilation flow rate, which is typically $\alpha \ll 1$ in office buildings, as must be assumed to derive equation (1). The general solution of equation (1) is

$$C(t) = C_\infty + (C_0 - C_\infty)e^{-\lambda t}, \quad (4)$$

where C_0 is the initial concentration at $t = 0$, and where the concentration C_∞ reached at times $t \gg \lambda^{-1}$ is given by

$$C_\infty - C_e = \frac{NqC_b}{xQ} = \alpha C_b. \quad (5)$$

Equations (2) and (5) show that both the equilibrium concentration difference $C_\infty - C_e$ and the characteristic time λ^{-1} needed to reach it are inversely proportional to xQ which, from a purely hygienic perspective, needs to be as high as possible to minimize the risk of airborne disease transmission. However, from an energy saving perspective, x and Q must remain reasonably low to minimize the energy cost of heating (in winter) or cooling down (in summer) the fresh outdoor air supplied to the room.

3. Materials and Methods

Experiments are performed in a so-called open plan office building in Wierden, Netherlands, consisting of a 435 m² open space with ceiling height 2.6 m sketched in Figure 2(c) which features the position of air supply and air exhaust vents. In this office, 20 to 40 employees from the company “Brand Builders,” male and female aged between 18 and 70, work with continuous communication with each other, which may include speaking with raised voices. Employees do not have any obligation to wear a face mask and are asked to keep windows and doors shut, regardless of weather conditions.

Air is supplied to the room via 25 supply vents placed in the ceiling and exhausted via 15 exhaust vents placed either in the ceiling, via open traps of the dropped ceiling, or near the floor via tubes carrying the air above the dropped ceiling. These two different air distribution strategies, labeled “overhead” and “downflow,” respectively, are sketched in Figures 1(b) and 1(c). In the overhead strategy, where the tubes are closed, the ceiling traps placed above these tubes are opened while, in the

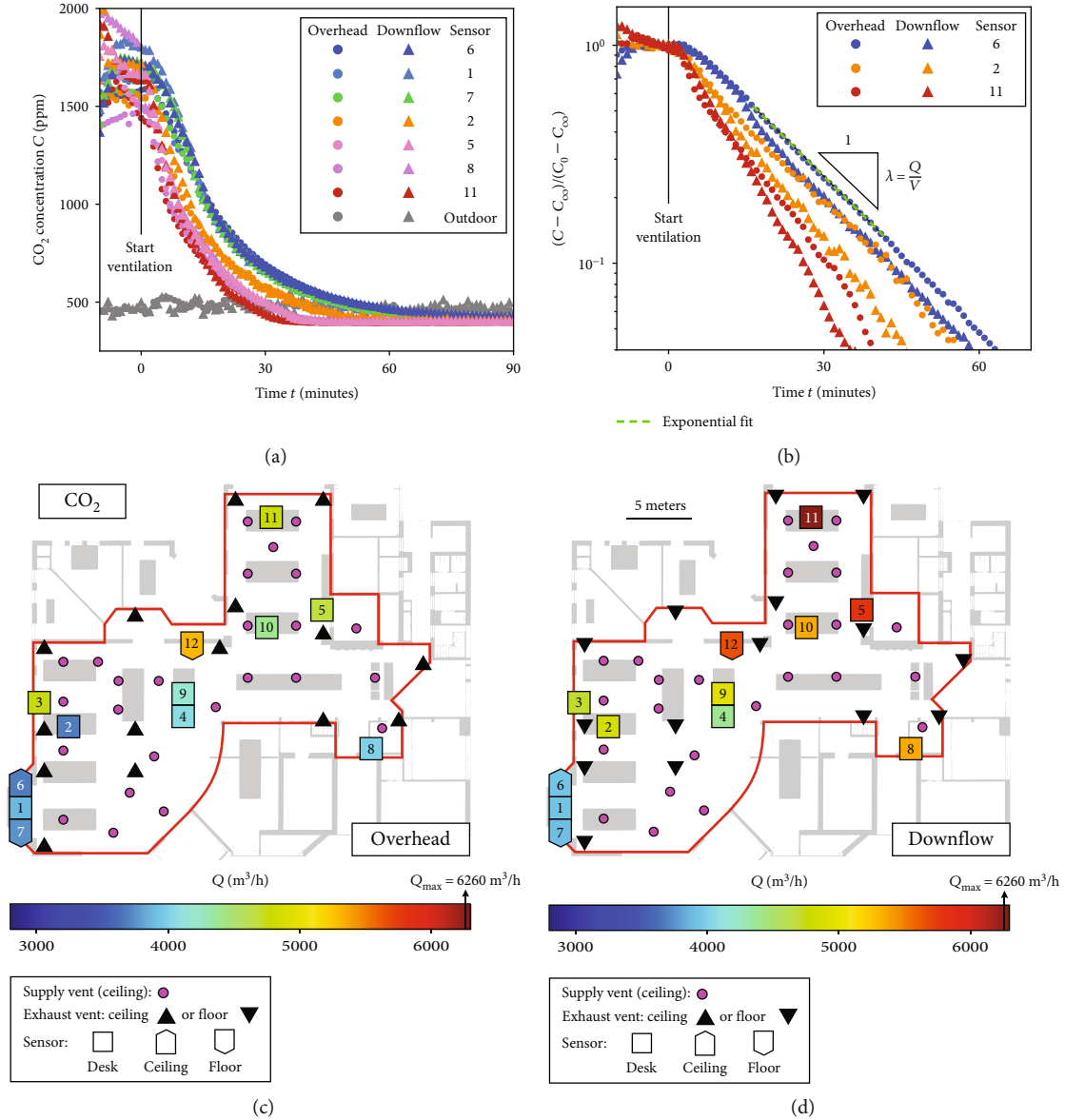


FIGURE 2: (a, b) Time evolution of the absolute (a) and renormalized (b) CO₂ concentration in a HADR experiment where ventilation is turned on at $t=0$, for different sensors for both overhead and downflow air distribution strategy. (c, d) Map of the effective flow rate Q measured for all sensors in overhead (c) and downflow (d) air distribution strategies. The zone outlined in red is the room where experiments were carried out; all doors leading to other rooms were closed. The position of supply vents in the ceiling, of exhaust vents in the ceiling (c) or near the floor (d), and of sensors at desk level or near the ceiling or floor is shown by symbols presented in the legend. The sensor symbols are colored based on their Q value following a code from blue (low Q) to red (high Q). A scale is shown in (d).

downflow strategy, all ceiling traps are closed and the tubes are open.

While breathing or speaking, humans produce aerosols as well as CO₂ which, when other potential sources are negligible, are good indexers of the indoor air quality. Hence, the office room in Wierden is equipped with 12 CO₂ (MH-Z19B) sensors and 5 air quality (SDS011) sensors placed on office desks and on the walls, either near the floor, at desk level, or near the ceiling. The air quality sensors measure the concentration of particulate matter of size less than 2.5 μm (PM_{2.5}) and less than 10 μm (PM₁₀) in the range 0-999.9 $\mu\text{g}/\text{m}^3$ with a precision of 0.3 $\mu\text{g}/\text{m}^3$. Addition-

ally, one CO₂ and one particle sensor are placed outside of the room to compare CO₂ and particle levels in the room with outdoor levels. We choose a time resolution of one data point per minute for all sensors.

A direct measurement of the flow rate delivered by each supply vent was performed using an anemometer, yielding a value of the total ventilation flow rate of $Q_{max} = 6260$ m³/h by summing over all supply vents. This value was measured at full ventilation capacity of the HVAC system. However, due to potential “shortcuts” between supply and exhaust vents, the effective air exchange rate λ might be less than the optimal value $\lambda_{max} = xQ_{max}/V$ expected from an ideal

ventilation capacity (see model in Section 2). This can be easily understood by considering that the CO₂ or aerosol concentration in the air exhausted via exhaust vents can indeed be lower than the average concentration across the room. Since the importance of these shortcuts depends on the position of the exhaust vents relative to the supply vents, different air distribution strategies are expected to yield different effective air exchange rates. In the following, results will be presented in terms of an effective flow rate $Q = \lambda V/x$ based on the measured CO₂ or aerosol elimination rate λ .

Two types of measurements are performed to estimate this effective available flow rate Q for both overhead and downflow air distribution strategies. The first consists of continuous measurements of the CO₂ and aerosol concentration in the room over several days between May and September 2022 and using the equilibrium concentration C_∞ to estimate Q for different air distribution strategies using equation (5), knowing the number of employees N in the rooms every day. These measurements are performed at full ventilation capacity with $x = 30\%$ of supplied outdoor air.

The second and more straightforward approach consists in partially filling the room with either CO₂ or aerosols at a sufficiently high initial concentration C_0 before turning the ventilation on at full capacity with a fraction $x = 100\%$ of outdoor supplied air (no recirculation) and without any employee in the room ($N = 0$), in which case, the concentration is expected to decrease exponentially from C_0 to C_e at a rate $\lambda = Q/V$ from which Q can be calculated (see the model in Section 2). These experiments will be referred to as HADR (hygienic air delivery rate) measurements as they aim at measuring the effective rate Q at which the air in a room is replaced by “fresh” air through the ventilation system. These HADR measurements were performed on Saturday, November 12th, 2022, for CO₂ and Saturday, September 3rd, 2022, for aerosols, testing both overhead and downflow air distribution strategies on the same day in both cases. For CO₂ measurements, the room was filled with CO₂ by sublimating a few kilograms of dry ice, pouring warm water on it to accelerate the sublimation process. For aerosol measurements, the room was filled with aerosols by spraying a liquid with a special spray nozzle provided by Medspray. The size distribution of droplets (before evaporation) and aerosols (after evaporation) was measured by a laser diffraction technique provided by Malvern Panalytical (Spraytec). The average droplet and aerosol diameters are 7 and 4 μm , respectively, when spraying at a flow rate of 34 ml/h, from which we estimate that $3 \cdot 10^9$ droplets/aerosols are produced per minute. The sprayed liquid consists of water with 1 wt% glycerin and 0.5 wt% NaCl so that, after water has evaporated, the glycerin and NaCl core remains in the form of an aerosol particle. Fans were used to homogenize the concentration during dry ice sublimation and aerosol spraying and were turned off before starting the experiments, i.e., before turning the ventilation system on.

The building’s HVAC system, which does not include a thermal wheel or HEPA filters, is equipped with an ultraviolet germicidal irradiation (UVGI) system provided by Virobuster placed before the outdoor air injection point so that recirculating indoor air is treated before reentering the room, as sketched in Figure 1(a). The UVGI module is about 1 m long

and exposes the circulating air to UV-C light of wavelength 254 nm with an intensity around 600 J/m². To test the efficiency of this technology on the air quality, air samples were collected every week on Friday morning between May and September 2022 (in parallel with continuous CO₂ and aerosol concentration measurements) by a certified validation company at five different locations across the room, the same locations every week, at heights 0.4 m, 0.75 m, and 2 m from the floor. The air sampling protocol consists of creating a 6 m³/h air flow through a Sartorius gelatin filter with 0.3 μm pores for 10 minutes during which employees were asked to not approach the sampling locations. Two additional air samples were collected, one outside to compare indoor air quality with outdoor and one in the air handling unit, after the UVGI module and before the outdoor air injection point, to check whether the air leaving the module is significantly affected by the UV-C treatment. The results for every sample are expressed in terms of a number of colony forming units (CFU), including both bacteria and fungi, the two being easily distinguishable. Measurements are organized in sets of at least two weeks corresponding to either overhead or downflow air distribution strategies, each strategy being tested with UVGI either turned on or turned off at full ventilation capacity with $x = 30\%$ of outdoor supplied air.

4. Results

4.1. HADR Experiments. The results of HADR measurements for CO₂ are presented in Figure 2(a) for both overhead and downflow distribution strategies where, starting from a high initial CO₂ concentration C_0 of ranging between 1500 and 2000 ppm, the concentration drops down to equilibrium values C_∞ around 400 ppm, close to the outdoor concentration. The rate at which the concentration decreases varies among different sensors placed at different locations across the room. Renormalized decay curves $(C - C_\infty)/(C_0 - C_\infty)$ are compared in Figure 2(b). We find that (i) the decay is exponential, in agreement with the model presented in Section 2, allowing measurement of the air exchange rate $\lambda = Q/V$ ($x = 1$ here since there is no indoor air recirculation) from which the effective flow rate Q is calculated for each sensor and that (ii) this effective flow rate is generally larger in downflow than in overhead. Only a few sensors representative of the range of Q values measured across the room are shown in Figures 2(a) and 2(b) for clarity. In Figure 2(b), we focus on the early times used for the exponential fit.

The difference between the two air distribution strategies is illustrated by the maps of Figures 2(c) and 2(d), showing the position of supply and exhaust vents in the room, as well as the position of CO₂ sensors which are colored based on their respective Q value in overhead (Figure 2(c)) and downflow (Figure 2(d)) strategies. We observe that the Q value measured for almost every sensor is larger in downflow than in overhead. The maps also reveal inhomogeneities, for example, with a less well ventilated region at the bottom left, with no significant differences between sensors placed at different heights.

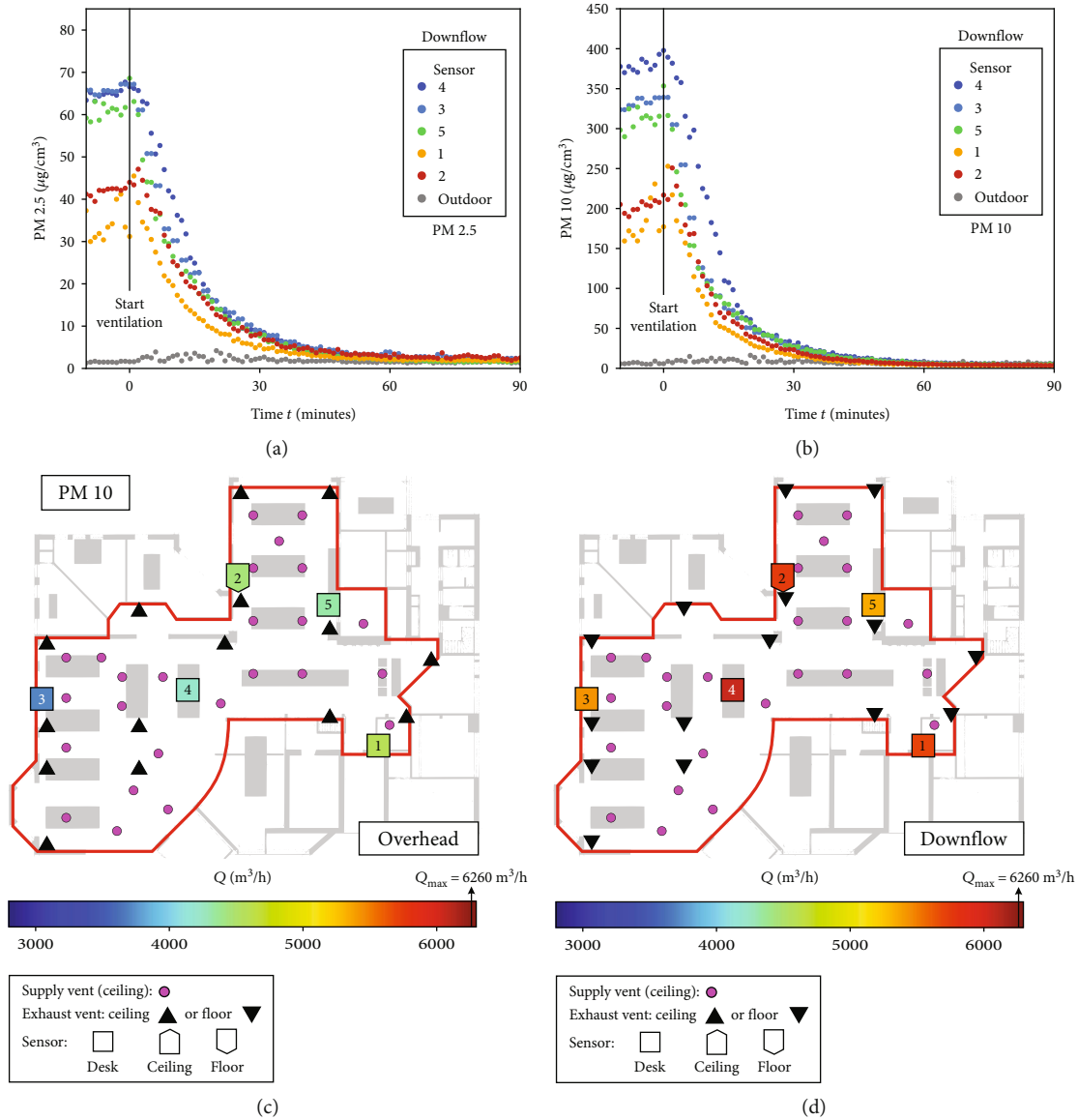


FIGURE 3: (a, b) Time evolution of the concentration of aerosols of size less than $2.5 \mu\text{m}$ (PM2.5) (a) and $10 \mu\text{m}$ (PM10) (b) in a HADR experiment where ventilation is turned on at $t=0$, for different sensors in a downflow air distribution strategy. (c, d) Map of the effective flow rate Q measured for all sensors in overhead (c) and downflow (d) air distribution strategies for aerosol of size less than $10 \mu\text{m}$ (PM10). The zone outlined in red is the room where experiments were carried out; all doors leading to other rooms were closed. The position of supply vents in the ceiling, exhaust vents in the ceiling (c) or near the floor (d), and sensors at desk level or near the ceiling or floor is shown by symbols presented in the legend. The sensor symbols are colored based on their Q value following a code from blue (low Q) to red (high Q).

Averaging over all sensors leads to effective flow rates $\langle Q \rangle = 4260 \text{ m}^3/\text{h}$ in overhead and $4930 \text{ m}^3/\text{h}$ in downflow with a standard variation of about $600 \text{ m}^3/\text{h}$ in both cases. These values are 32% and 21% smaller than the maximum flow rate Q_{max} that would be reached in the absence of shortcuts in the air flow, respectively, meaning that adopting a downflow air distribution strategy reduces the importance of these shortcuts by improving the effective average available flow rate $\langle Q \rangle$ by 16% compared to overhead.

Similar results are found for aerosol HADR measurements, as shown in Figures 3(a) and 3(b) presenting the decay curves of the concentration in aerosols of size less than

$2.5 \mu\text{m}$ (PM2.5) and $10 \mu\text{m}$ (PM10), respectively, in a downflow air distribution strategy. Note that the initial concentration C_0 reached before turning the ventilation on is larger for PM10 than for PM2.5, meaning that the spraying technique used to fill the room with aerosols produces more particles of size larger than $2.5 \mu\text{m}$. As shown in the maps of Figures 3(c) and 3(d), like for CO_2 , the effective flow rate Q calculated from these exponential decay curves is larger in downflow than in overhead for all sensors. Averaging over all sensors leads to effective flow rates $\langle Q \rangle = 4180 \text{ m}^3/\text{h}$ in overhead and $5390 \text{ m}^3/\text{h}$ in downflow for PM2.5 and $\langle Q \rangle = 4240 \text{ m}^3/\text{h}$ in overhead and $5660 \text{ m}^3/\text{h}$ in downflow

TABLE 1: Effective flow rates Q measured from HADR measurements (no employees in the room) with CO_2 and aerosols (PM2.5 and PM10) and from continuous CO_2 measurements (employees in the room) for overhead and downflow air distribution strategies. The last line shows the improvement of downflow compared to overhead in percentage. In the absence of shortcuts, the measured flow rate should be equal to the optimal value $Q_{\max} = 6260 \text{ m}^3/\text{h}$ measured with an anemometer.

	HADR CO_2	Cont. CO_2	HADR PM2.5	HADR PM10
Q_{\max} (m^3/h)-optimal	6260	6260	6260	6260
Q (m^3/h)-(O)verhead	4260	4260	4180	4240
Q (m^3/h)-(D)ownflow	4930	4670	5390	5660
% improvement O to D	16	10	29	33

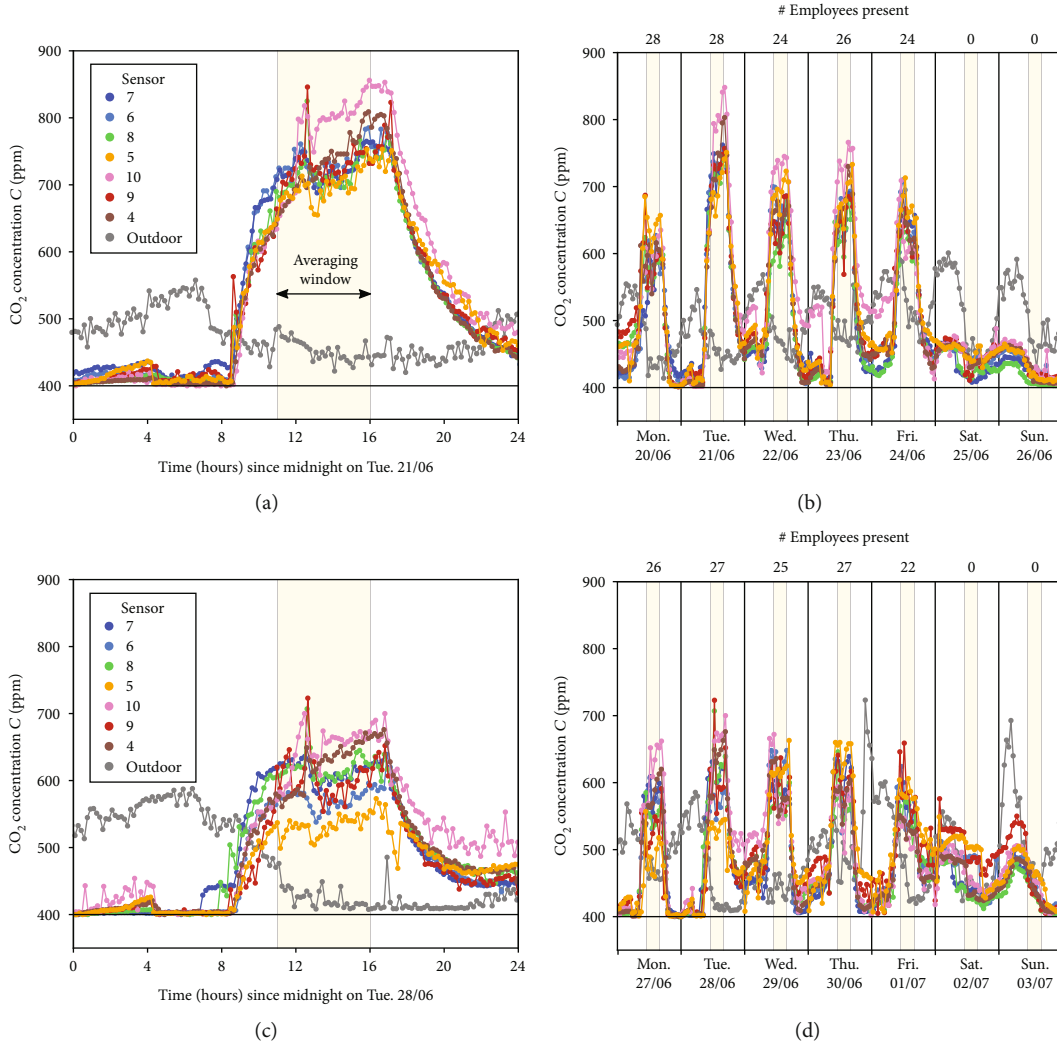
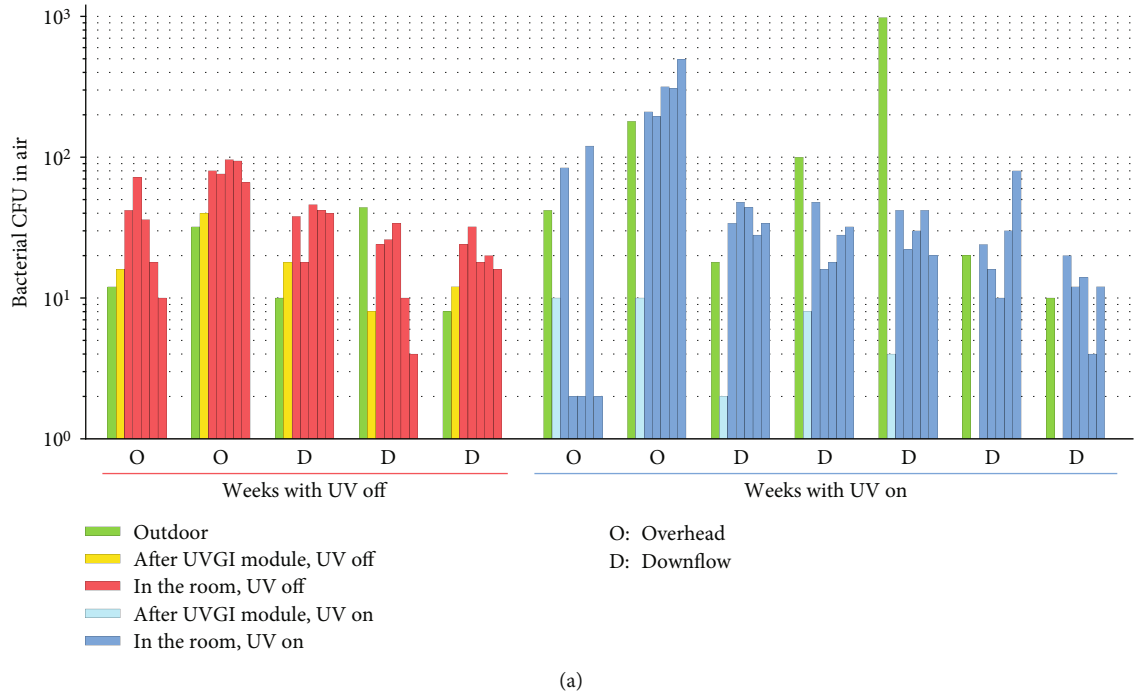


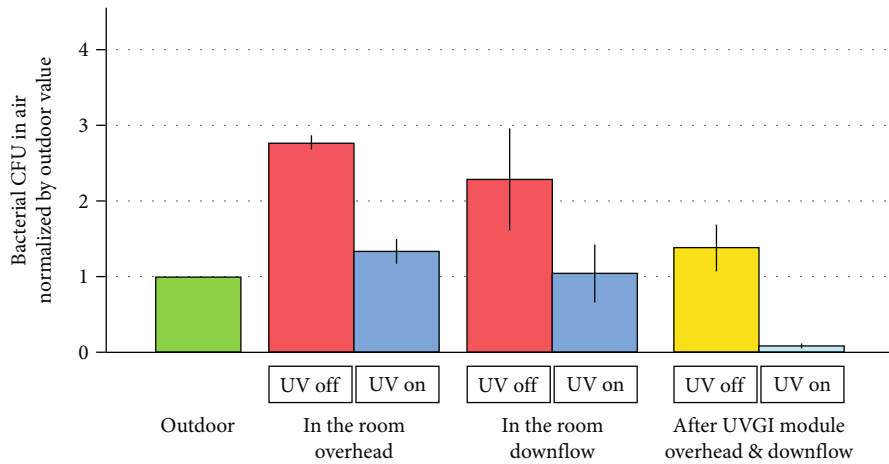
FIGURE 4: Time evolution of the CO_2 concentration in the room for different sensors over one working day (a, c) and one full week (b, d) with overhead (a, b) and downflow (c, d) ventilation strategies. The number of employees present in the room every day is indicated in the top x -axis in (b) and (d) which correspond to two consecutive weeks from June 20th to June 26th (b) and from June 27th to July 3rd (d) and (a) and (c) corresponding to Tuesday of each of these two weeks. The equilibrium concentration C_{∞} is calculated by averaging over all indoor sensors between 11 am and 4 pm. While the real time resolution is one data point per minute, we only show enough points to see the trend in this figure.

for PM10, with standard variations of about $400 \text{ m}^3/\text{h}$ in all four cases. This means that adopting a downflow air distribution strategy improves the effective flow rate by about 30% for aerosols, compared to overhead, which is a more pronounced improvement than for CO_2 .

Flow rates and improvement percentages are presented in Table 1. The more pronounced improvement observed for aerosols compared to CO_2 suggests that, in addition to the reduction in air shortcuts between supply and exhaust vents affecting both CO_2 and aerosols, a downflow air



(a)



(b)

FIGURE 5: (a) Number of bacteria CFU, in log scale, measured outdoor (green), at five locations inside the room (red or blue) and just after the UVGI module (yellow or cyan) for 5 weeks where UVGI was turned off (red and yellow) and 7 weeks where it was turned on (blue and cyan), each case being tested with overhead (O) and downflow (D) air distribution strategies. (b) Averaged bacteria CFU normalized by the outdoor value, in lin scale, with the same color code as in (a). Error bars correspond to the standard variation over different weeks.

distribution strategy also enhances the elimination rate of aerosols via a second aerosol-specific mechanism. A possible interpretation is that, when being forced towards the floor, aerosols are more likely to be deposited on surfaces as they encounter more obstacles such as tables, chairs, and other furniture, which would also occur in the absence of ventilation due to gravitational sedimentation [49].

4.2. Continuous Concentration Measurements. The time evolution of the CO_2 concentration during normal working days with employees present in the room is shown over one day (Figures 4(a) and 4(c)) and over one week (Figures 4(b) and 4(d)) for an overhead (Figures 4(a) and 4(b)) and downflow (Figures 4(c) and 4(d)) air distribution

strategy. The indoor concentration starts increasing at around 8 am and start decreasing at around 5 pm, consistent with typical working hours, while the outdoor CO_2 concentration increases slightly during the night and decreases in the morning, consistent with the plant breathing cycle (CO_2 release during the night and capture during the day). We can therefore correlate the indoor CO_2 concentration with the presence of people. However, as shown in Figures 4(b) and 4(d) where the number of employees present each day is indicated on the top x -axis, the indoor CO_2 concentration does not correlate perfectly with the number of employees present, probably due to some employees partially working outside of the main room where the concentration was measured (i.e., outside of the region outlined in

red in Figures 2(c) and 2(d) and 3(c) and 3(d)). For that reason, estimating the effective flow rate for the two air distribution strategies using equation (5), where C_{∞} is estimated by averaging between 11 am and 4 pm, averaging over several days for each strategy, yields significant standard deviations. Using $C_b = 40,000$ ppm and $q = 220$ l/h gives average values $\langle Q \rangle = 4260$ m³/h in overhead and 4670 m³/h in downflow with standard variations of about 1300 m³/h in both cases, which is larger than the 10% improvement of downflow compared to overhead estimated from these values, shown in Table 1. We therefore believe that HADR measurements are a more reliable way to measure the effective flow rate and to detect differences between different air distribution strategies.

Our measurements show that the average aerosol concentration was typically between 3 and 6 $\mu\text{g}/\text{m}^3$ for PM10 and between 1 and 3 $\mu\text{g}/\text{m}^3$ for PM2.5, for all sensors, both on weekends and working days; the variations are due to the variations in outdoor fine dust concentrations. During working days, we observe peaks up to 20 $\mu\text{g}/\text{m}^3$ (PM10) and 8 $\mu\text{g}/\text{m}^3$ (PM2.5) lasting less than 20 minutes appearing on different sensors at different times; these are likely due to people producing aerosols. However, not enough aerosols were produced to significantly raise the average aerosol concentration above the background value, and we concluded that the CO₂ concentration was better correlated with the presence of people in the room. We consequently decided to not use our continuous aerosol measurements to estimate the effective flow rate, but rather the continuous CO₂ measurements.

4.3. Effect of Ultraviolet Germicidal Irradiation. The results of the air quality measurements carried out on Friday every week are shown in Figure 5(a) where the number of bacteria colony forming units (CFU) is measured outdoor (green), at five locations inside the room (red or blue) and just after the UVGI module (yellow or cyan) is shown for 5 weeks where UVGI was turned off (red and yellow) and 7 weeks where it was turned on (blue and cyan), each case being tested with overhead and downflow air distribution strategies. We observe strong variations of both outdoor and indoor air qualities between different weeks, with numbers of bacteria CFU ranging typically between 10 and 1000 for outdoor air samples. This is not surprising since the presence of bacteria in the air is expected to depend on the temperature and relative humidity [74, 75]. Days of high outdoor bacterial concentration also show high indoor bacterial concentration when the UVGI module was off. Hence, for every measurement day, we normalize the indoor air quality, quantified by the number of bacteria CFU, measured at different locations in the room and after the UVGI module, by the outdoor air quality. Strong air quality variations are observed for different air sampling locations in the room for a given day, the location of the worst measured air quality not being the same every week. This is not surprising since the amount of bacteria in the air at a given location can vary significantly depending on the presence of nearby sources such as plants or food whose location can vary from day to day. Hence, we average over all five locations in the room for every measurement day to obtain an average room air quality.

The final results are presented in Figure 5(b) where the air quality in the room and after the UVGI module is compared to the outdoor air quality. We average over weeks corresponding to the same air distribution strategy (overhead or downflow) for the air quality in the room and over all weeks for the air quality after the UVGI module, distinguishing in both cases between weeks where the UVGI was turned on (blue and cyan) and weeks where it was turned off (red and yellow). The error bars represent the variation over different weeks. These results show a strong improvement of the air quality in the room when UVGI is turned on, typically by a factor two, making indoor air almost as clean as outdoor. This is confirmed by the sharp reduction in bacterial count after the UVGI module when it is turned on. No significant difference is measured between the two air distribution strategies.

5. Conclusions and Discussions

Our experiments confirm that ultraviolet germicidal irradiation (UVGI) technologies can significantly improve the indoor air quality in buildings when indoor air is partly reinjected in the room via recirculation, bringing the level of active airborne bacteria almost as low as in the outdoor air. Since viruses are much weaker than bacteria and since the UV-C intensity of around 600 J/m² of the UVGI technology used in this study surpasses the required 90% inactivation energy of SARS-CoV-2 (27 J/m² [46]), it can be assumed that the level of active airborne viruses will also be significantly reduced after UVGI treatment. Hence, assuming a virus-free outdoor air, the risk of airborne contamination is significantly reduced. We therefore conclude that energy saving requirements, from which air recirculation is encouraged, can be reconciled with hygienic requirements when properly treating the air reinjected in the building.

The effective flow rate Q , or equivalently the effective air exchange rate λ , available to replace indoor air with “clean” (outdoor or treated indoor) air was shown to be systematically less than the flow rate expected from direct measurements of supply vent delivery. This is caused by “shortcuts” in the global air flow of the room between supply and exhaust vents, which cause the air being exhausted to be more similar to the clean supplied air than to the average air in the room, either in terms of CO₂ or aerosol concentration or, consequently, in terms of temperature and humidity. While air bacterial concentration measurements did not allow us to rank the two different air distribution strategies tested (overhead and downflow), a clear improvement of up to 30% was measured in the effective air flow rate Q for downflow compared to overhead, proving that supply-exhaust air shortcuts can be significantly minimized by changing the air distribution strategy. Future work is needed to characterize the optimal position of inlet and exhaust vents to minimize these shortcuts and to compare a downflow situation to the reverse case (not considered in the present study) where air is supplied from the floor and exhausted from the ceiling.

The improvement in ventilation capacity implies that, in addition to a better protection against virus-laden aerosols, a better air distribution strategy is also beneficial in terms of

energy savings. Indeed, for example, in winter, the presence of supply-exhaust shortcuts means that a fraction of the precious warm air supplied to the room is directly thrown away into exhaust vents before properly mixing in the room. Hence, when limiting these shortcuts, less ventilation energy is needed to keep the indoor air temperature at a prescribed value, which has a significant economic impact. In other words, an optimal air distribution strategy can lead to the same indoor air quality as for another (less optimal) strategy, both in terms of temperature and aerosol safety, with less ventilation power. For example, on a 4°C winter day with 100% outdoor air supply (no indoor air recirculation), the thermal power needed to warm the outdoor air flowing in the air handling unit at flow rate $Q_{\max} = 6260 \text{ m}^3/\text{h}$ up to 21°C is 35 kW based on the density and specific heat capacity of air. Once in the room, our effective flow rate measurements in “overhead” showed that about 30% of the flow rate is lost due to shortcuts, implying a power loss of about 11 kW. In contrast, in “downflow,” based on CO₂ and aerosol measurements, only 20% to 10% of the flow rate is lost, respectively, implying a power loss of only 7.4 kW to 3.5 kW.

We note that the use of UVGI modules in HVAC systems could, in principle, allow the use of rotary heat wheels, since the deactivation of pathogens that, without treatment, would be reinjected in the building via the “carry-over effect”, could ensure an acceptable indoor air quality. Moreover, in contrast to air filters, UVGI modules can be easily switched on when required and do not introduce any additional pressure drop in the air handling unit (AHU). This solution is therefore not only ecologically justifiable but also economically viable. In principle, UVGI modules also allow the use of cheap and small AHU without separated exhaust and supply air, i.e., without rotary heat wheels. This is particularly interesting since these ventilation systems allow, via indoor air recirculation, an easier regulation of the indoor air humidity, especially in winter, with the associated benefits for occupants’ well-being.

Data Availability

The data used to support the findings of this study are available from the corresponding authors upon request.

Disclosure

This manuscript was submitted as a preprint in the link “<https://europepmc.org/article/ppr/ppr609953>” [76].

Conflicts of Interest

The authors declare no conflicts of interest.

Acknowledgments

The authors would like to thank Sander G. Huisman for the fruitful discussions. The authors acknowledge funding by the NWO (Dutch Research Council) under the MIST (Mitigation Strategies for Airborne Infection Control) program.

References

- [1] L. Bourouiba, “Turbulent gas clouds and respiratory pathogen emissions,” *JAMA*, vol. 323, pp. 1837–1838, 2020.
- [2] S. L. Miller, W. W. Nazaroff, J. L. Jimenez et al., “Transmission of SARS-CoV-2 by inhalation of respiratory aerosol in the Skagit Valley chorale superspreading event,” *Indoor Air*, vol. 31, no. 2, pp. 314–323, 2021.
- [3] G. Buonanno, L. Stabile, and L. Morawska, “Estimation of airborne viral emission: quanta emission rate of SARS-CoV-2 for infection risk assessment,” *Environment International*, vol. 141, article 105794, 2020.
- [4] G. A. Somsen, C. van Rijn, S. Kooij, R. A. Bem, and D. Bonn, “Small droplet aerosols in poorly ventilated spaces and sars-cov-2 transmission,” *The Lancet Respiratory Medicine*, vol. 8, no. 7, pp. 658–659, 2020.
- [5] M. Abkarian, S. Mendez, N. Xue, F. Yang, and H. A. Stone, “Speech can produce jet-like transport relevant to asymptomatic spreading of virus,” *Proceedings of the National Academy of Sciences*, vol. 117, no. 41, pp. 25237–25245, 2020.
- [6] F. Yang, A. A. Pahlavan, S. Mendez, M. Abkarian, and H. A. Stone, “Towards improved social distancing guidelines: space and time dependence of virus transmission from speech-driven aerosol transport between two individuals,” *Physical Review Fluids*, vol. 5, no. 12, article 122501, 2020.
- [7] C. van Rijn, G. A. Somson, L. Hofstra et al., “Reducing aerosol transmission of SARS-CoV-2 in hospital elevators,” *Indoor Air*, vol. 30, no. 6, pp. 1065–1066, 2020.
- [8] M. Z. Bazant and J. W. Bush, “A guideline to limit indoor airborne transmission of COVID-19,” *Proceedings of the National Academy of Sciences*, vol. 118, no. 17, article e2018995118, 2021.
- [9] L. Bourouiba, “The fluid dynamics of disease transmission,” *Annual Review of Fluid Mechanics*, vol. 53, no. 1, pp. 473–508, 2021.
- [10] K. L. Chong, C. S. Ng, N. Hori, R. Yang, R. Verzicco, and D. Lohse, “Extended lifetime of respiratory droplets in a turbulent vapor puff and its implications on airborne disease transmission,” *Physical Review Letters*, vol. 126, no. 3, article 034502, 2021.
- [11] C. S. Ng, K. L. Chong, R. Yang, M. Li, R. Verzicco, and D. Lohse, “Growth of respiratory droplets in cold and humid air,” *Physical Review Fluids*, vol. 6, no. 5, article 054303, 2021.
- [12] G. Bagheri, B. Thiede, B. Hejazi, O. Schlenczek, and E. Bodenschatz, “An upper bound on one-to-one exposure to infectious human respiratory particles,” *Proceedings of the National Academy of Sciences*, vol. 118, no. 49, article e2110117118, 2021.
- [13] M. L. Pöhlker, O. O. Krüger, J. D. Förster et al., “Respiratory aerosols and droplets in the transmission of infectious diseases,” 2021, <http://arxiv.org/abs/2103.01188>.
- [14] F. Poydenot, I. Abdourahmane, E. Caplain et al., “Risk assessment for long- and short-range airborne transmission of SARS-CoV-2, indoors and outdoors,” *PNAS Nexus*, vol. 1, no. 5, 2022.
- [15] B. Mutsch, M. Heiber, F. Grätz et al., “Aerosol particle emission increases exponentially above moderate exercise intensity resulting in superemission during maximal exercise,” *Proceedings of the National Academy of Sciences*, vol. 119, no. 22, article e2202521119, 2022.
- [16] W. J. Fisk, “Health and productivity gains from better indoor environments and their relationship with building energy

- efficiency,” *Annual Review of Energy and the Environment*, vol. 25, no. 1, pp. 537–566, 2000.
- [17] Y. Li, G. M. Leung, J. W. Tang et al., “Role of ventilation in airborne transmission of infectious agents in the built environment—a multidisciplinary systematic review,” *Indoor Air*, vol. 17, no. 1, pp. 2–18, 2007.
- [18] WHO, *Q&A: Ventilation and Air Conditioning in Public Spaces and Buildings and COVID-19*, Tech. Rep. World Health Organization, 2020.
- [19] L. Morawska, J. W. Tang, W. Bahnfleth et al., “How can airborne transmission of COVID-19 indoors be minimised?,” *Environment International*, vol. 142, article 105832, 2020.
- [20] L. Morawska and J. Cao, “Airborne transmission of SARS-CoV-2: the world should face the reality,” *Environment International*, vol. 139, article 105730, 2020.
- [21] M. Jayaweera, H. Perera, B. Gunawardana, and J. Manatunge, “Transmission of COVID-19 virus by droplets and aerosols: a critical review on the unresolved dichotomy,” *Environmental Research*, vol. 118, article 109819, 2020.
- [22] K. A. Prather, C. C. Wang, and R. T. Schooley, “Reducing transmission of SARS-CoV-2,” *Science*, vol. 368, no. 6498, pp. 1422–1424, 2020.
- [23] V. Stadnytskyi, C. E. Bax, A. Bax, and P. Anfinrud, “The airborne lifetime of small speech droplets and their potential importance in SARS-CoV-2 transmission,” *Proceedings of the National Academy of Sciences*, vol. 117, no. 22, pp. 11875–11877, 2020.
- [24] R. Zhang, Y. Li, A. L. Zhang, Y. Wang, and M. J. Molina, “Identifying airborne transmission as the dominant route for the spread of COVID-19,” *Proceedings of the National Academy of Sciences*, vol. 117, no. 26, pp. 14857–14863, 2020.
- [25] T. Greenhalgh, J. L. Jimenez, K. A. Prather, Z. Tufekci, D. Fisman, and R. Schooley, “Ten scientific reasons in support of airborne transmission of SARS-CoV-2,” *The Lancet*, vol. 397, no. 10285, pp. 1603–1605, 2021.
- [26] CDC, “Ventilation in Buildings,” Tech. Rep. Centers for Disease Control and Prevention, 2021.
- [27] L. Morawska, J. Allen, W. Bahnfleth et al., “A paradigm shift to combat indoor respiratory infection,” *Science*, vol. 372, no. 6543, pp. 689–691, 2021.
- [28] D. Tsai, J. Lin, and C. Chan, “Office workers’ sick building syndrome and indoor carbon dioxide concentrations,” *Journal of Occupational and Environmental Hygiene*, vol. 9, no. 5, pp. 345–351, 2012.
- [29] J. Dreier, A. Bermpohl, P. Jeschin, B. Becker, and K. Kleesiek, “Transmission von viren durch raumluftechnische anlagen und inaktivierung durch uvc-strahlung,” *Gefahrstoffe-Reinhal-tung der Luft*, vol. 68, no. 9, p. 379, 2008.
- [30] C. J. Simonson, *Heat and Moisture Transfer in Energy Wheels, [Ph.D. thesis]*, University of Saskatchewan Saskatoon, SK, Canada, 1998.
- [31] G. Alshami, “Rotary heat exchangers for Heat Recovery in Ventilation Systems Handbook for Design, Installation and Operation,” 2018, , https://www.academia.edu/13225470/Rotary_heat_exchangers_for_Heat_Recovery_in_Ventilation_Systems_Handbook_for_Design_Installation_and_Operation.
- [32] H. M. D. P. Herath, M. D. A. Wickramasinghe, A. M. C. K. Polgolla, A. S. Jayasena, R. A. C. P. Ranasinghe, and M. A. Wijewardane, “Applicability of rotary thermal wheels to hot and humid climates,” *Energy Reports*, vol. 6, pp. 539–544, 2020.
- [33] A. Schwartz, M. Stiegel, N. Greeson et al., “Decontamination and reuse of n95 respirators with hydrogen peroxide vapor to address worldwide personal protective equipment shortages during the sars-cov-2 (covid-19) pandemic,” *Applied Biosafety*, vol. 25, no. 2, pp. 67–70, 2020.
- [34] A. Filipić, I. Gutierrez-Aguirre, G. Primc, M. Mozetič, and D. Dobnik, “Cold plasma, a new hope in the field of virus inactivation,” *Trends in Biotechnology*, vol. 38, no. 11, pp. 1278–1291, 2020.
- [35] A. Lai, A. Cheung, M. Wong, and W. Li, “Evaluation of cold plasma inactivation efficacy against different airborne bacteria in ventilation duct flow,” *Building and Environment*, vol. 98, pp. 39–46, 2016.
- [36] F. J. Garcia de Abajo, R. J. Hernández, I. Kaminer, A. Meyerhans, J. Rosell-Llompart, and T. Sanchez-Elsner, “Back to normal: an old physics route to reduce sars-cov-2 transmission in indoor spaces,” *ACS Nano*, vol. 14, no. 7, pp. 7704–7713, 2020.
- [37] M. L. Hitchman, “A new perspective of the chemistry and kinetics of inactivation of COVID -19 coronavirus aerosols,” *Future Virology*, vol. 15, no. 12, pp. 823–835, 2020.
- [38] G. Somsen and D. Bonn, “Infection control unit suppresses airborne aerosols during cardiac stress testing in an outpatient cardiology clinic,” *Journal of Clinical and Experimental Cardiology*, vol. 12, p. 692, 2021.
- [39] B. Blocken, T. van Druenen, A. Ricci et al., “Ventilation and air cleaning to limit aerosol particle concentrations in a gym during the covid-19 pandemic,” *Building and Environment*, vol. 193, article 107659, 2021.
- [40] D. Hart, “Bactericidal ultraviolet radiation in the operating room: twenty-nine-year study for control of infections,” *Journal of the American Medical Association*, vol. 172, no. 10, pp. 1019–1028, 1960.
- [41] W. Kowalski, “UVGI disinfection theory,” in *Ultraviolet germicidal irradiation handbook*, pp. 17–50, Springer, 2009.
- [42] D. Menzies, J. Popa, J. A. Hanley, T. Rand, and D. K. Milton, “Effect of ultraviolet germicidal lights installed in office ventilation systems on workers’ health and wellbeing: double-blind multiple crossover trial,” *The Lancet*, vol. 362, no. 9398, pp. 1785–1791, 2003.
- [43] D. Sharp, “The lethal action of short ultraviolet rays on several common pathogenic bacteria,” *Journal of Bacteriology*, vol. 37, no. 4, pp. 447–460, 1939.
- [44] C. Tseng and C. Li, “Inactivation of virus-containing aerosols by ultraviolet germicidal irradiation,” *Aerosol Science and Technology*, vol. 39, no. 12, pp. 1136–1142, 2005.
- [45] C. M. Walker and G. Ko, “Effect of ultraviolet germicidal irradiation on viral aerosols,” *Environmental Science & Technology*, vol. 41, no. 15, pp. 5460–5465, 2007.
- [46] W. Kowalski, T. Walsh, and V. Petraitis, *Covid-19 coronavirus ultraviolet susceptibility*, Purplesun Inc, 2020.
- [47] W. Chen, N. Zhang, J. Wei, H.-L. Yen, and Y. Li, “Short-range airborne route dominates exposure of respiratory infection during close contact,” *Building and Environment*, vol. 176, article 106859, 2020.
- [48] L. Bourouiba, E. Dehandschoewercker, and J. W. Bush, “Violent expiratory events: on coughing and sneezing,” *Journal of Fluid Mechanics*, vol. 745, pp. 537–563, 2014.
- [49] S. H. Smith, G. A. Somsen, C. van Rijn et al., “Aerosol persistence in relation to possible transmission of SARS-CoV-2,” *Physics of Fluids*, vol. 32, no. 10, article 107108, 2020.

- [50] M. Liu, J. Liu, Q. Cao et al., "Evaluation of different air distribution systems in a commercial airliner cabin in terms of comfort and COVID-19 infection risk," *Building and Environment*, vol. 208, article 108590, 2022.
- [51] A. F. El-Haroun, S. A. Kaseb, M. A. Fouad, and H. O. Kayed, "Numerical investigation of covid-19 infection spread expelled from cough in an isolation ward under different air distribution strategies," *Journal of Advanced Research in Fluid Mechanics and Thermal Sciences*, vol. 95, no. 1, pp. 17–35, 2022.
- [52] Y. Zhang, G. Feng, Z. Kang, Y. Bi, and Y. Cai, "Numerical simulation of coughed droplets in conference room," *Procedia Engineering*, vol. 205, pp. 302–308, 2017.
- [53] C. H. Cheong, B. Park, and S. R. Ryu, "Effect of under-floor air distribution system to prevent the spread of airborne pathogens in classrooms," *Case Studies in Thermal Engineering*, vol. 28, article 101641, 2021.
- [54] M. Abdolzadeh, E. Alimolaei, and M. Pustelnik, "Numerical simulation of airflow and particle distributions with floor circular swirl diffuser for underfloor air distribution system in an office environment," *Environmental Science and Pollution Research*, vol. 26, no. 24, pp. 24552–24569, 2019.
- [55] T. N. Verma, A. K. Sahu, and S. L. Sinha, "Study of particle dispersion on one bed hospital using computational fluid dynamics," *Materials Today: Proceedings*, vol. 4, no. 9, pp. 10074–10079, 2017.
- [56] C. Xu, X. Wei, L. Liu et al., "Effects of personalized ventilation interventions on airborne infection risk and transmission between occupants," *Building and Environment*, vol. 180, article 107008, 2020.
- [57] F. H. Shair and K. L. Heitner, "Theoretical model for relating indoor pollutant concentrations to those outside," *Environmental Science & Technology*, vol. 8, no. 5, pp. 444–451, 1974.
- [58] M. E. Davis and R. J. Davis, *Fundamentals of Chemical Reaction Engineering*, Courier Corporation, 2012.
- [59] W. F. Wells, *Airborne Contagion and Air Hygiene: An Ecological Study of Droplet Infections*, Harvard University Press, Cambridge, MA, 1955.
- [60] E. Riley, G. Murphy, and R. Riley, "Airborne spread of measles in a suburban elementary school," *American Journal of Epidemiology*, vol. 107, no. 5, pp. 421–432, 1978.
- [61] Y. Shah, J. W. Kurelek, S. D. Peterson, and S. Yarusevych, "Experimental investigation of indoor aerosol dispersion and accumulation in the context of covid-19: effects of masks and ventilation," *Physics of Fluids*, vol. 33, no. 7, article 073315, 2021.
- [62] J. Howard, A. Huang, Z. Li et al., "An evidence review of face masks against COVID-19," *Proceedings of the National Academy of Sciences*, vol. 118, no. 4, article e2014564118, 2021.
- [63] N. H. L. Leung, D. K. W. Chu, E. Y. C. Shiu et al., "Respiratory virus shedding in exhaled breath and efficacy of face masks," *Nature Medicine*, vol. 26, no. 5, pp. 676–680, 2020.
- [64] W. Yang and L. C. Marr, "Dynamics of airborne influenza A viruses indoors and dependence on humidity," *PLoS One*, vol. 6, no. 6, article e21481, 2011.
- [65] G. Buonanno, L. Morawska, and L. Stabile, "Quantitative assessment of the risk of airborne transmission of sars-cov-2 infection: prospective and retrospective applications," *Environment International*, vol. 145, article 106112, 2020.
- [66] M. Z. Bazant, O. Kodio, A. E. Cohen, K. Khan, Z. Gu, and J. W. Bush, "Monitoring carbon dioxide to quantify the risk of indoor airborne transmission of COVID-19," *Flow*, vol. 1, p. E10, 2021.
- [67] Z. Peng and J. L. Jimenez, "Exhaled CO₂ as a COVID-19 infection risk proxy for different indoor environments and activities," *Environmental Science & Technology Letters*, vol. 8, no. 5, pp. 392–397, 2021.
- [68] L. Stabile, A. Pacitto, A. Mikszewski, L. Morawska, and G. Buonanno, "Ventilation procedures to minimize the airborne transmission of viruses in classrooms," *Building and Environment*, vol. 202, article 108042, 2021.
- [69] W. R. von Pohle, J. D. Anholm, and J. McMillan, "Carbon dioxide and oxygen partial pressure in expiratory water condensate are equivalent to mixed expired carbon dioxide and oxygen," *Chest*, vol. 101, no. 6, pp. 1601–1604, 1992.
- [70] S. N. Rudnick and D. K. Milton, "Risk of indoor airborne infection transmission estimated from carbon dioxide concentration," *Indoor Air*, vol. 13, no. 3, pp. 237–245, 2003.
- [71] K. Lin and L. C. Marr, "Humidity-dependent decay of viruses, but not bacteria, in aerosols and droplets follows disinfection kinetics," *Environmental Science & Technology*, vol. 54, no. 2, pp. 1024–1032, 2020.
- [72] L. C. Marr, J. W. Tang, J. Van Mullekom, and S. S. Lakdawala, "Mechanistic insights into the effect of humidity on airborne influenza virus survival, transmission and incidence," *Journal of The Royal Society Interface*, vol. 16, no. 150, article 20180298, 2019.
- [73] G. Harper, "Airborne micro-organisms: survival tests with four viruses," *Epidemiology & Infection*, vol. 59, no. 4, pp. 479–486, 1961.
- [74] P. Hoeksma, A. J. A. Aarnink, and N. W. M. Ogink, "Effect of temperature and relative humidity on the survival of airborne bacteria= effect van temperatuur en relatieve luchtvochtigheid op de overleving van bacteriën in de lucht," Tech. Rep. Wageningen UR Livestock Research, 2015.
- [75] Y. Qiu, Y. Zhou, Y. Chang et al., "The effects of ventilation, humidity, and temperature on bacterial growth and bacterial genera distribution," *International Journal of Environmental Research and Public Health*, vol. 19, no. 22, p. 15345, 2022.
- [76] A. Gaillard, D. Lohse, D. Bonn, and F. Yigit, "Reconciling airborne disease transmission concerns with energy saving requirements: the potential of UV-C pathogen deactivation and air distribution optimization," 2023, <https://europepmc.org/article/PPR/PPR609953>.